

Figure S1. Alignment of the amino acid sequences for the Arabidopsis VAMP proteins. Identical residues for VAMP721, VAMP722, and VAMP723 highlighted in grey and key residues identified in the central longin domain are boxed in red.

Longin Domain	
VAMP711	MAILYALVARGTVVLFSEFTATSTNASTIAKQILEKVPDGN-DSNVSYSDRYVHFVKRTDGLT-----
VAMP712	MSILYALVARGTVVLAELSTTSTNASTIAKQILEKIPNGN-DSHVSYSQDRYVHFVKRTDGLT-----
VAMP713	MAIIFALVARGTVVLFSEFSATSTNASSISKQILEKLPGNDSHMSYSQDRYIFHFVKRTDGLT-----
VAMP714	MAIVYAVVARGTVVLAEFSAVTGNTGAVVRRILEKLSPEISDERLCFSQDRYIFHILRSDGLT-----
VAMP721	M <sup>57</sup> AQQSLIYSEFVARGTVILVEFTDFKGNFTSIAAQCLQKLPSSN-N-KFTYNCDGHTFNYLVLDGFT-----
VAMP722	M <sup>61</sup> AQQSLIYSEFVARGTVILVEFTDFKGNFTSIAAQCLQKLPSSN-N-KFTYNCDGHTFNYLVENGESSESKEYCSIS
VAMP723	M <sup>57</sup> AQQSLFYSFIARGTVILVEFTDFKGNFTSIAAQYLENLPSSN-N-KFTYNCDGHTFNDLVENGFT-----
VAMP724	M <sup>66</sup> GQESFIYSFVARGTMI LAEYTEFTGNFPSIAAQCLQKLPSSS-NSKFTYNCDHHTFNFVLDVGYA-----
VAMP725	M <sup>66</sup> GQQLIYSFVARGTVILVEYTEFKGNFTAVAAQCLQKLPSSN-N-KFTYNCDGHTFNYLVENGFT-----
VAMP726	M <sup>66</sup> GQSLIYSFVARGTVILAEYTEFKGNFTSVAQCLQKLPSSN-N-KFTYNCDGHTFNYLVADNGFT-----
VAMP727	M <sup>66</sup> SQGLIYSFVARGTVVLAEHPTYSGNFSTIAVQCLQKLPSTNS-S-KYTYSCDGHTFNFVLDVNGFV-----
VAMP728	-----MVVDRNGYNYLTQQ-----
Longin Domain	
VAMP711	VLCMAEETAGRRI PF AFLEDIHQRFVRTYGRAVHT-----ALAYAMNEEFSRVLSSQIDYY
VAMP712	VLCMADEDAGRRI PF SFLEDIHQRFVRTYGRAIHS-----AQAYAMNDEFSRVLNQIEYY
VAMP713	VLCMADETAGRNIPF AF LDDIHQRFVKTYGRAIHS-----AQAYSMNDEFSRVLSSQMEFY
VAMP714	FLCMANDTFGRRVPFYSYLEEIHMRFMKNYGKVAHN-----APAYAMNDEFSRVLHQQMEFF
VAMP721	YCVVAVDSAGRQIPMSF <sup>76</sup> FLERVKEDFN <sup>80</sup> KRYGGGKAAT-----AQANSLNKEFGSKLKEHMQYC
VAMP722	YCVVAVDSAGRQIPMAFLERVKEDFNKRYGGGKAAT-----AQANSLNKEFGSKLKEHMQYC
VAMP723	YCVVAVDSAGREIPMAFLERVKEDFYKRYGGGKAAT-----DQANSLNKEFGSNLKEHMQYC
VAMP724	YCVVAKDSLKQISIAFLERVKADFKRYGGGKAST-----AIAKSLNKEFGPVMKEHMNYI
VAMP725	YCVVAVESVGRQIPMAFLERVKEDFNKRYGGGKATT-----AQANSLNREFGSKLKEHMQYC
VAMP726	YCVVIESAGRQIPMAFLERVKEDFNKRYGGGKAST-----AKANSLNKEFGSKLKEHMQYC
VAMP727	FLVVADESTGRSVPPVFLERVKEDFKRYEASIKNDERHPLADEDDEDDDFGDRFSVAYNLDREFGPI LKEHMQYC
VAMP728	-----LEQRVLVL
R-SNARE	
VAMP711	SNDP-NADRINRIK GEMNQVRGMVMIENIDKVLDRGERLELLVDK---TAN---MQGNTFRFRKQARRFRSNVWWRN
VAMP712	SNDP-NADTISRIGEMNQVRDVMVMIENIDNILDGRGERLELLVDK---TAN---MQGNTFRFRKQTRRRFNNTVWWRN
VAMP713	SNDP-NADRMSRIK GEMSQVRNVMVMIENIDKVLDRGERLELLVDK---TEN---MQGNTFRFRKQARRYRTIMWWRN
VAMP714	SSNP-SVDTLNRVRGEVSEIRSMVVENIEKIMERGDRIELLVDK---TAT---MQDSSFHFRKQSKRLRRALWMKN
VAMP721	MDHPDEISK <sup>76</sup> LAKVKAQVSEVKG <sup>80</sup> VMMENIEKVLDRGEKIELLVDK---TENL--RSQAQ-DFRTGTQMRKRMWLFON
VAMP722	MDHPDEISK <sup>76</sup> LAKVKAQVSEVKG <sup>80</sup> VMMENIEKVLDRGEKIELLVDK---TENL--RSQAQ-DFRTGTQMRKRMWLFON
VAMP723	MDHPDEISNLAKAKAQVSEVKS <sup>76</sup> LMMENIEKVLARGVIC <sup>80</sup> EMIGS---SE---SQPO-AEYIKR <sup>76</sup> TOMKRRK <sup>80</sup> WLFON
VAMP724	VDHAEIEKLIKVKVKAQVSEVKSIMLENIDKVIDRGENLTVLTDK---TENL--RSQAR-EYKQGTQVRRKRLWYQN
VAMP725	VDHPDEISKLAKVKAQVTEVKGMMENIEKVLDRGEKIELLVDK---TENL--RSQAQ-DFRTGTQKIRKRMWFEN
VAMP726	ADHPDEISKLSKVKVKAQVTEVKGMMENIEKVLDRGEKIELLVDK---TENL--RSQAQ-DFRTGTQKMRKRLWFEN
VAMP727	MSHPDEISKLSKLAQITEVKGIMMDNIEKVLDRGEKIELLVDK---TENL--QFQAD-SFQQRGRLRRKMWLQS
VAMP728	LAHPDEISKLAKVKALVTMKVGMENIEKALDRSEKIKILVLDLRSKYSNLPFPYSYGQEDIITPGTKITRKMWFQN
TM helices	
VAMP711	CKLTVLLILLLLVIIYIAVAFCHGPTLPSCI.
VAMP712	CKLTLLLLILVLLVIIYGVAFACHGPTLPSCV.
VAMP713	VKLTIALILVLLVVIYIAMAFCVCHGPTLPSCFK.
VAMP714	LVLTLCLIVFLLYIIIASFCGGITLPSCRS.
VAMP721	MKIKLIVLAI <sup>76</sup> IIALILII <sup>80</sup> ILSV <sup>76</sup> CHGFK <sup>80</sup> C.
VAMP722	MKIKLIVLAI <sup>76</sup> IIALILII <sup>80</sup> ILSI <sup>76</sup> CGGFN <sup>80</sup> CGK.
VAMP723	MKIKLIVLAI <sup>76</sup> IIALILII <sup>80</sup> ILSV <sup>76</sup> CGGFN <sup>80</sup> CGK.
VAMP724	MKIKLVVLGILLLLVIIWISVCHGFNCTD.
VAMP725	MKIKLIVLGIITLILIIILSVCGGFKCT.
VAMP726	MKIKLIVFGIIVALILIIILSVCHGFKCT.
VAMP727	LQMKLMVAGAVFSFILIVVAVACGGFKCSS.
VAMP728	MKFKLIVLGTSSSRFVLITERRRR-LR.

Figure S2. VAMP721, but not VAMP723, interacts with the KC1 K<sup>+</sup> channel in vivo. rBiFC analysis of nYFP-VAMP fusions of VAMP721 and VAMP723 and their interaction with KC1-cYFP. Images were collected from Arabidopsis roots epidermal cells transiently transformed as in Figure 2. Three-dimensional projections were derived from confocal image stacks and the projections were analysed for YFP and RFP fluorescence intensities after background subtraction. Images are (*left to right*) YFP (BiFC) fluorescence, RFP fluorescence as a cell marker, and the corresponding mid-plane brightfield image. The images correspond to constructs (*top to bottom*) including the coding sequences for KC1-cYFP with the empty cassette (control), VAMP721, and VAMP723. Scale bar, 10  $\mu$ m. Immunoblot analysis verifying the expression of the fusion proteins are included on the right. Mean  $\pm$ SE for rBiFC ratios (YFP/RFP fluorescence) comprise data from three independent experiments, each including images ( $n > 10$ ) taken from randomly selected roots. rBiFC fluorescence ratios were calculated from the mean fluorescence intensities determined from each YFP/RFP image pair after background subtraction. Significance is indicated by letters ( $P < 0.01$ ).

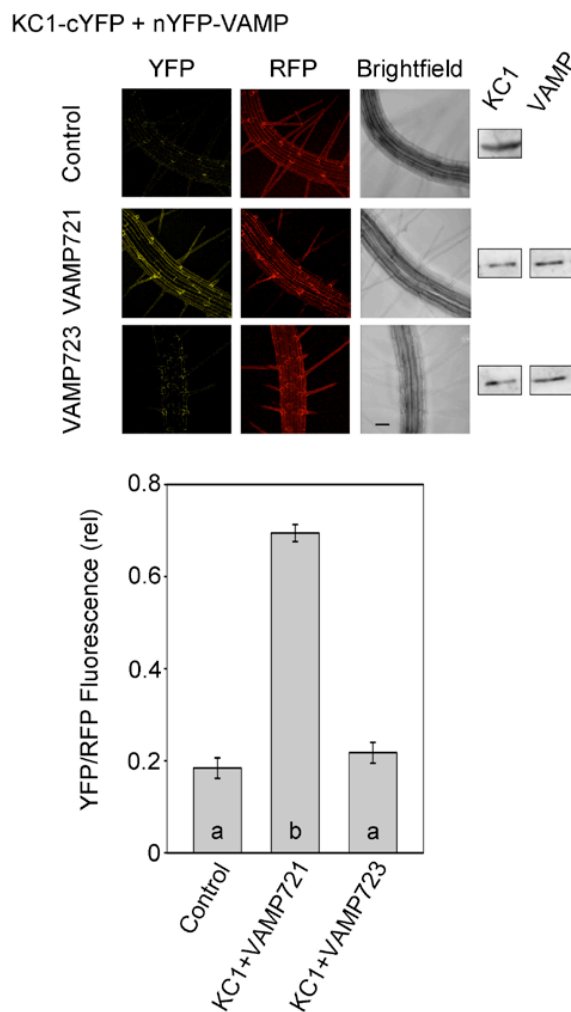


Figure S3. The central section of the VAMP721 Longin Domain is essential for interaction with KAT1.

Yeast mating-based split-ubiquitin assay for interaction of the VAMP longin domain chimeras with KAT1-Cub as the bait. Longin domain chimeras were constructed by exchange of three segments designated L<sub>A</sub>, L<sub>B</sub>, and L<sub>C</sub>. Chimeras were constructed both in VAMP721 and VAMP723. Segment alignments (above) for the two VAMPs at the junction points are shown with arrows indicating the breaks. Yeast diploids created with NubG fusion constructs of each VAMP chimeras together with controls (negative, NubG; positive, wild-type Nub[Nubl]) spotted (left to right) on CSM medium without Leu, Trp, Ure, and Met (CSM<sub>-LTUM</sub>) to verify mating, CSM medium without Leu, Trp, Ure, Met, Ade, and His (CSM<sub>-LTUMAH</sub>) to verify adenine- and His-independent growth (second panel), and on CSM<sub>-LTUMAH</sub> with the addition of 50  $\mu$ M Met to verify interaction at lower KAT1-Cub expression levels (Grefen et al., 2009). Diploid yeast was dropped at 1.0 and 0.1 OD600 in each case. Immunoblot analysis (5  $\mu$ g total protein/lane) of the haploid yeast used for mating is included (right) using commercial HA antibody for VAMPs and and VP16 antibody for K<sup>+</sup> channels.

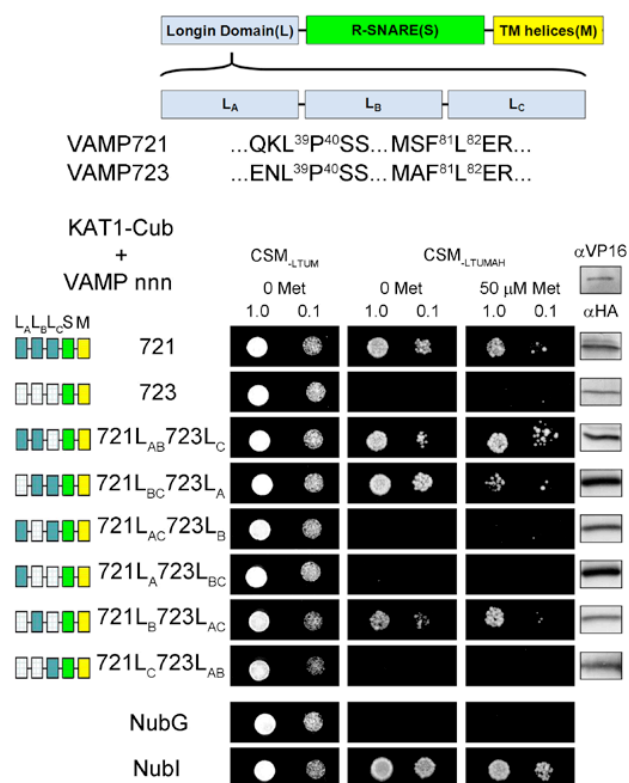


Figure S4. Single-site mutants VAMP721<sup>D61N</sup>, VAMP721<sup>Y57F</sup> and VAMP721<sup>Q76E</sup> have no substantive effect on interaction with KAT1 or KC1, and AKT1 shows no interaction with VAMP721 or VAMP723.

Yeast mating-based split-ubiquitin assay for interaction of VAMPs with KAT1-Cub (A), KC1-Cub (B), and AKT1-Cub (C) as baits. Yeast diploids were created with NubG fusion constructs of each of the VAMP proteins together with controls [NubG, negative; Nubl (wild-type), positive] spotted (*left to right*) on CSM medium without Leu, Trp, Ura, and Met (CSM<sub>-LTUM</sub>) to verify mating, CSM medium without Leu, Trp, Ura, Met, Ade, and His (CSM<sub>-LTUMAH</sub>) to verify adenine- and His-independent growth, and on CSM<sub>-LTUMAH</sub> with the addition of Met to verify interaction at lower K<sup>+</sup> channels-Cub expression levels (50  $\mu$ M for KAT1 and AKT1, 500  $\mu$ M for KC1). Diploid yeast was dropped at 1.0 and 0.1 OD<sub>600</sub> in each case. Immunoblot analysis (5  $\mu$ g total protein/lane) of the haploid yeast used for mating (*right*) using commercial HA antibody for the VAMP fusions and VP16 antibody for the K<sup>+</sup> channel fusions.

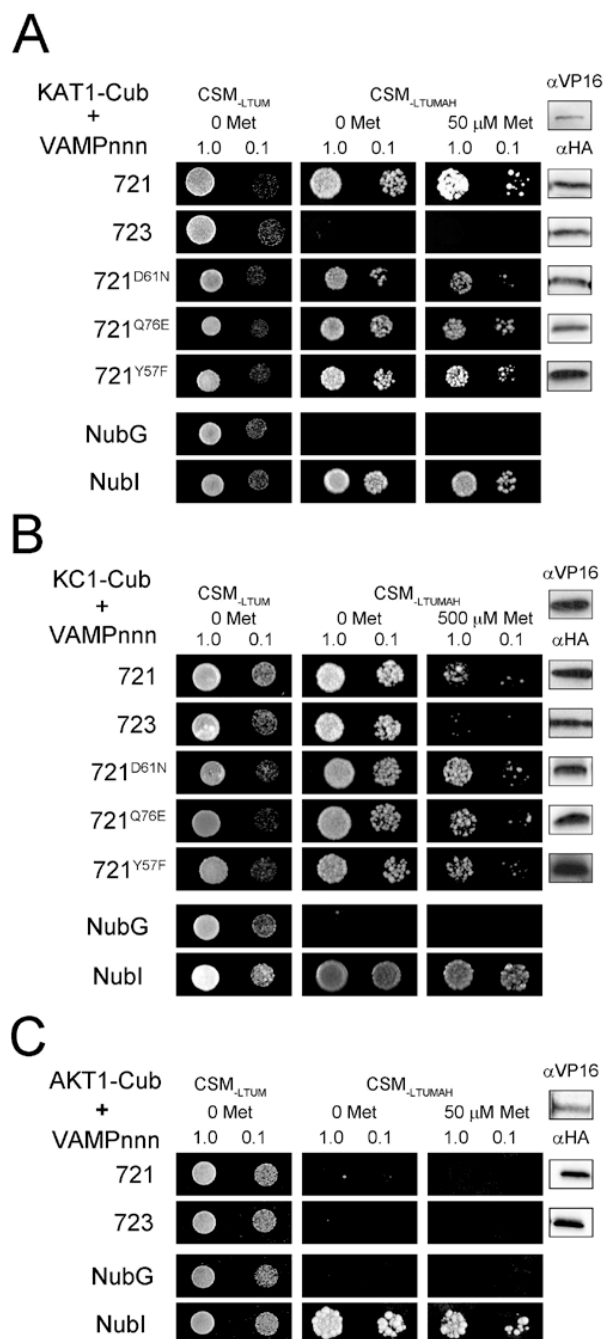


Figure S5. The VAMP721<sup>Y57D</sup> mutant suppresses interaction with the KC1 K<sup>+</sup> Channel. Yeast mating-based split-ubiquitin assay for interaction of single-site mutants of VAMP721 with KAT1-Cub as bait. Yeast diploids were created with NubG fusion constructs of each of the VAMP proteins together with controls [NubG, negative; Nubl (wild-type), positive] spotted (*left to right*) on CSM medium without Leu, Trp, Ura, and Met (CSM<sub>-LTUM</sub>) to verify mating, CSM medium without Leu, Trp, Ura, Met, Ade, and His (CSM<sub>-LTUMAH</sub>) to verify adenine- and His-independent growth, and on CSM<sub>-LTUMAH</sub> with the addition of Met to verify interaction at lower K<sup>+</sup> channels-Cub expression levels. Diploid yeast was dropped at 1.0 and 0.1 OD<sub>600</sub> in each case. Immunoblot analysis (5 μg total protein/lane) of the haploid yeast used for mating (*right*) using commercial HA antibody for the VAMP fusions and VP16 antibody for the K<sup>+</sup> channel fusion.

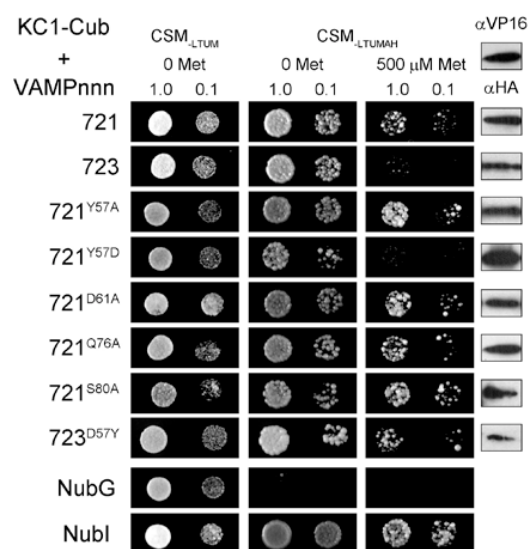


Figure S6. The single-site mutants VAMP721<sup>Y57D</sup> and VAMP723<sup>D57Y</sup> affect the localization of the R-SNAREs.

Images showing (*left to right*) optical sections through Arabidopsis root hairs with GFP fluorescence, bright-field and overlay, and with Z-axis transects (panels 1-4) for GFP-tagged constructs of VAMP721, VAMP721<sup>Y57D</sup>, VAMP723, and VAMP723<sup>D57Y</sup>. The GFP-VAMP constructs were transiently transformed in Arabidopsis seedlings and images collected 3 d post-transformation. Transects were taken through the root hair nucleus at positions marked in the overlap images (1-4 from *top to bottom*) in each example. No GFP signal was observed to the inside of the nucleus for GFP-VAMP721 and GFP-VAMP723<sup>D57Y</sup>, indicating a peripheral localization. GFP fluorescence was evident to the inside of the nucleus (*white arrows*) on transformations with GFP-VAMP721<sup>Y57D</sup> and GFP-VAMP723, consistent with the localization of the constructs to one or more endomembrane compartments. Scale bar, 5  $\mu$ m.

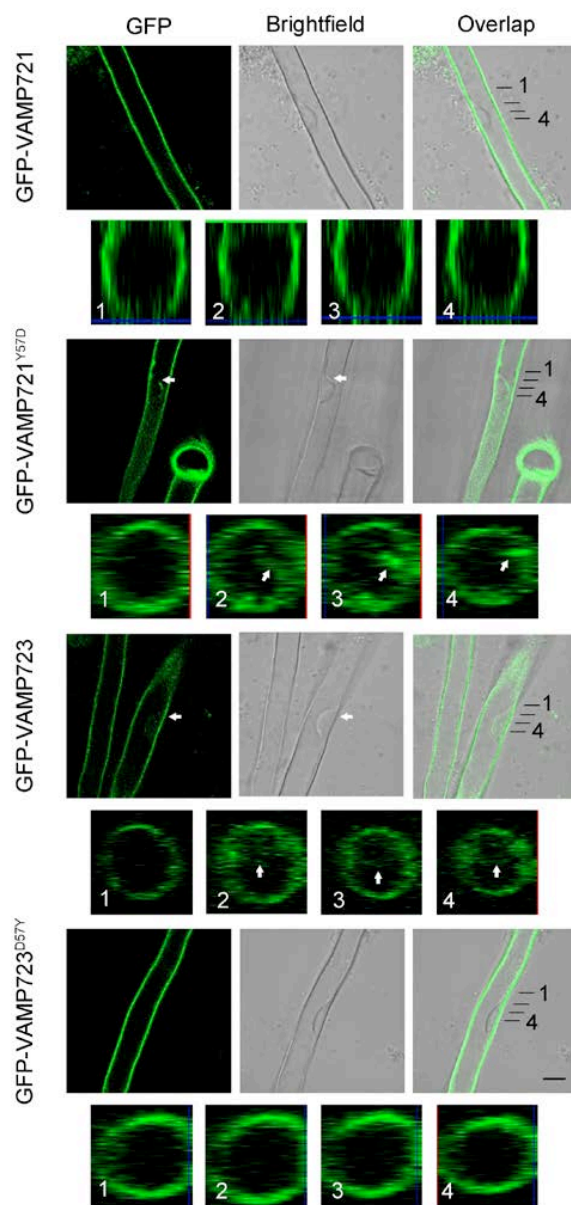


Figure S7. Arabidopsis lines carrying VAMP721 VAMP723 and VAMP721<sup>Y57D</sup> under the Dex-inducible promoter show no substantive effects on root growth dependent on channel-mediated K<sup>+</sup> uptake at submillimolar K<sup>+</sup> in the absence of dexamethasone.

(A) Arabidopsis seedlings grown for 10 d on vertical 0.7% agar plates with defined minimal salts medium containing 0.01, 0.1 and 1 mM K<sup>+</sup> with 2 mM NH<sub>4</sub><sup>+</sup> to block high-affinity K<sup>+</sup> uptake. Shown are seedlings of wild-type (wt) and representative Arabidopsis transgenic lines. Scale bar, 1 cm.

(B) Root length analysis of Arabidopsis seedlings for wt and pooled lines carrying the VAMP721, VAMP723, and VAMP721<sup>Y57D</sup> constructs, including the seedlings in (A). Data are means  $\pm$ SE from three independent experiments with >20 seedlings for each line normalized to the wild-type. Root lengths for lines of each transgene have been pooled and are normalized to the wild-type at the same K<sup>+</sup> concentration. Lines are not significantly different at P<0.1. Immunoblot analysis for transgene expression are included in Figure 12.

